approximate the R/C ratio, dealing with a compound and corrected for self-absorption, to the very simple relationship:

$$\left(\frac{R}{C}\right)_{eff} = \left[\sum_1^m w_i \left(\frac{R}{C}\right)_i\right] \cdot F(w_1, w_2, \ldots) \qquad (3)$$

where the sum is extended to the m different chemical elements characterizing the compound, and F is a correction function (≥ 1) dealing with the self-absorption process. Also in this case a XRF contribution improves the evaluation.

In Fig. 9 the calculated $(R/C)_{eff}$ values are compared with experimental values dealing with low Z compounds.

In order to give a complete picture of the RCT properties in the analysis of compounds we point out that, as shown in Fig. 4 for pure elements, it is not possible to define a simple relationship between R/C and Z in all the Z range but the approximation

$$R/C = a\, Z^n \qquad (4)$$

can be written and the full Z range must be divided in two or more regions dealing with different n's ($2{,}2 \leqslant n \leqslant 4$). When the elements of a compound are clustered in only one of these regions it is always possible to define a Z effective of the sample according to the relationship:

$$Z_{eff} = \left[\sum_1^m w_i Z_i^n\right]^{1/n} \qquad (5)$$

Equation (5) turns out to be particularly useful when a fast evaluation of the chemical characteristics of a material is requested. A better evaluation will be done afterwards through the XRF–RCT system when it is possible.

It must be pointed out that Z_{eff} is quite different from Z because the former is strictly related to equation (4).

In order to demonstrate the equation (4) is quite a good approximation we have reported in Fig. 10 the behaviour of R/C vs a calculated Z_{eff}. The R/C experimental points refer to Au alloys. One can see the experimental points fit very well with the theoretical ones, putting $n = 2.2$ in equation (4).

Discussion

The RCT gives a further improvement in the fast non-destructive analyses concerning materials of technological interest.

In general RCT turns out to be more flexible than the XRF technique, even if less sensitive, because the latter is strongly limited both by fluorescence line self-absorption and by the increasing inefficiency of the detector at very low x-ray energies. A more appropriate choice of E_0 and ϑ can always be made whenever RCT is expressly devoted to solving a particular problem.

In concluding, the XRF–RCT spectrometer we have developed for *in situ* rapid first approach analyses can be employed in material testing problems in chemistry, geology, biology, archaeometry and medicine, for example. The multipurpose system capability can be synthesized, by the block diagram reported in Fig. 11, in which are shown the procedures to be followed and the different steps to be pursued when an *a priori* first simple identification of the material nature is given.

References

1. Bertin E. P. *Principles and Practice of X-ray Spectrometric Analysis* (Plenum Press, New York, 1975).
2. Cesareo R., Frazzoli F. V. and Sciuti S. *J. Radioanal. Chem.* **34**, 157 (1976).
3. McKenzie I. M. *Nucl. Instrum. Methods* **49**, 162 (1979).
4. Zumzendorf H. *Nucl. Instrum. Methods.* **98**, 611 (1972).
5. Schotzler H. P. *Int. J. Appl. Radiat. Isot.* **30**, 115 (1975).
6. Cesareo R., Ferretti M. and Marabelli M. *Archaeometry* **24**, 170 (1982).
7. Notea A. and Segal Y. *Nucl. Technol.* **34**, 73 (1974).
8. Hubbell J. H. *et al. J. Phys. Chem. Ref. Data* **4**, 471 (1975); see also Hubbell J. H. and Overbo I. *ibid.* **8**, 69 (1979).

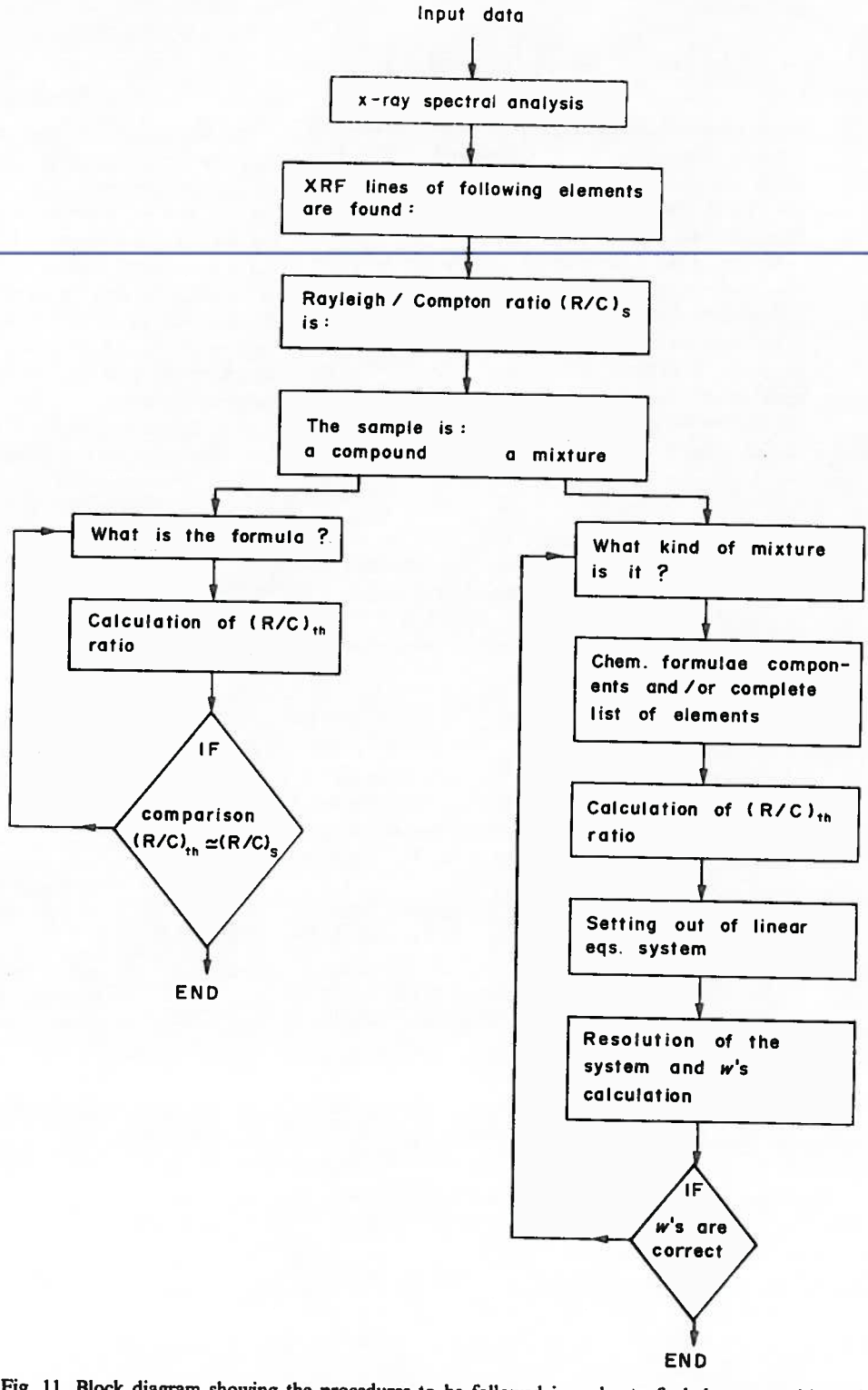

Fig. 11. Block diagram showing the procedures to be followed in order to find the composition of a material when a hypothesis on the material nature can be given. w's are the weight fractions of the various components (elements or compounds).

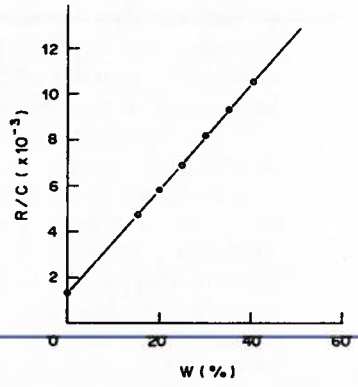

Fig. 7. R/C values for $Ca_3(PO_4)_2$ in glycerine vs the $Ca_3(PO_4)_2$ weight fraction w (in %).

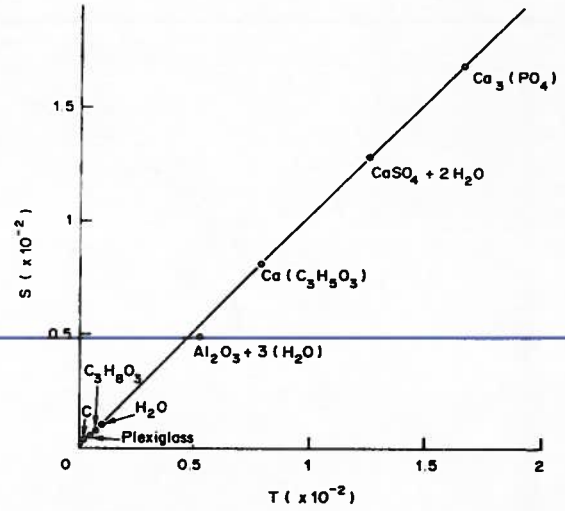

Fig. 9. Measured R/C ratios, S, for low-Z elements and compounds vs calculated effective R/C ratios, T, as from equation (3).

sensitive and accurate analyses as is found for binary and ternary alloys. For binary alloys the following two equations are contemporary satisfied:

$$R/C = a_0 + a\ w \tag{1}$$

$$I_{XRF} = b_0 + b\ w \tag{1'}$$

where R/C is the Rayleigh to Compton ratio, I_{XRF} is the intensity of the higher energy fluorescence line and w is the weight fraction of the corresponding element.

For ternary alloys the following linear system of equations can be written:

$$\begin{aligned} R/C &= a_0 + a_1\ w_1 + a_2\ w_2 \\ I_{XRF} &= b_0 + b_1\ w_1 + b_2\ w_2 \end{aligned} \tag{2}$$

where the w's are the weight fractions of two elements over three chosen as follows:

—one deals with the higher energy fluorescence line;
—the other is the major component of the alloy.

In the cases in which samples of indefinible shape and thickness must be measured, the R/C value is still appropriate while the XRF intensity could be substituted by the ratio I_{XRF}/C. The value C, which is the Compton intensity, can be intended as an approximate normalizing geometrical and physical parameter.

In Fig. 8 the Ag–Cu alloy calibration curve is reported; a 1% sensitivity can be easily achieved with a reasonable measuring time.

The RCT turns out to be very useful for rigorous alloy control related to deeper layer inspections and to the detection of contaminations, if not less than 1%, of light elements such as oxygen, carbon etc. not detectable by XRF.

The RCT applies also to the determination of any chemical compound because it is always possible to

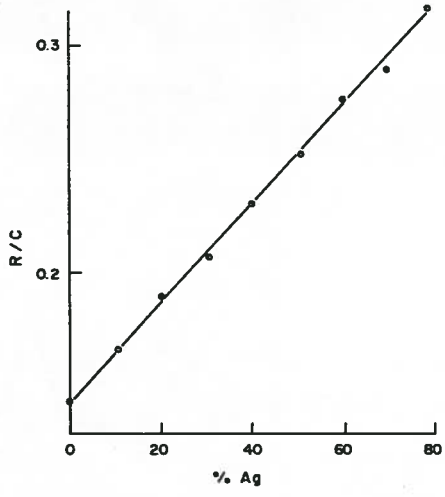

Fig. 8. R/C values for Ag–Cu alloys vs Ag weight fraction w (in %).

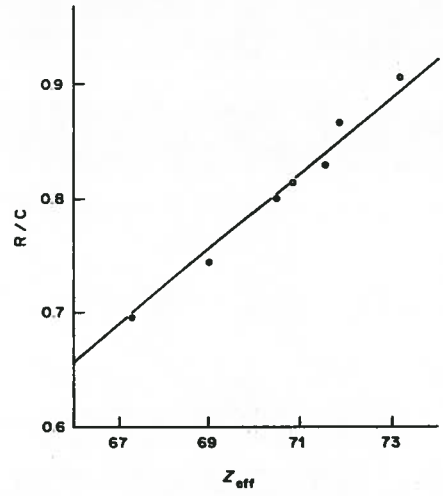

Fig. 10. R/C measured values vs calculated Z_{eff}, as from equation (5) for $n = 2.2$. The experimental values refer to some standard Au alloys.

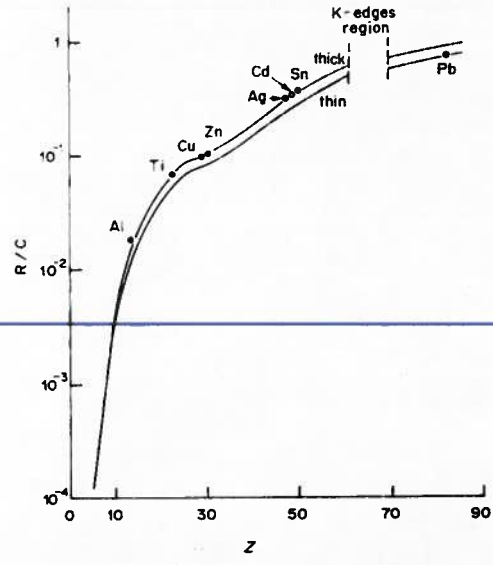

Fig. 4. Calculated R/C values vs the atomic number Z at $E_0 = 59.5$ keV and $\vartheta = 135°$. The reported experimental points are in good agreement with the calculated ones.

sample mean atomic number $\bar{Z}$ increases, as is shown in Fig. 5 where the sample thickness ρx, i.e. the critical value starting from which the sample must be considered "thick", is plotted vs Z. Therefore the thickness related to the measured area variates for some centimeters (free air) to $\sim 500\,\mu$m (high absorbing media): in any case we can assume that the RCT involves volume measurements instead of surface measurements as done by XRF.

The strong dependence of the analyzed effective volume depth upon self-absorption is clearly shown in Fig. 6: a high Compton peak corresponds to a low-Z matrix (Fig. 6a), while for high-Z materials (Fig. 6b) the peak is strongly reduced. It must be pointed out that the very good Compton profile symmetry is to be related to a small angular spread around the scattering angle and consequently to a well defined illuminated volume.

From Fig. 4 one can deduce that even when fluorescence lines are absent in the spectrum (low-Z elements) it is still possible to formulate an hypothesis about the sample composition. Further, a quantitative evaluation can be made if an *a priori* list of elements composing the sample is available. For instance, in the case of mixtures of chemical elements or compounds constituted by low-Z elements only ($Z \leqslant 15$) it is possible to simulate the sample composition though a binary system and finally to calculate its real composition. For example in Fig. 7 a R/C calibration curve for a two-component system, i.e. tricalcium phosphate in glycerine is reported. It is possible to evaluate $Ca_3\,(PO_4)_2$ variations less than 1% in 400 s measuring time.

If the spectrum contains XRF lines it is possible to combine the two techniques in order to have more

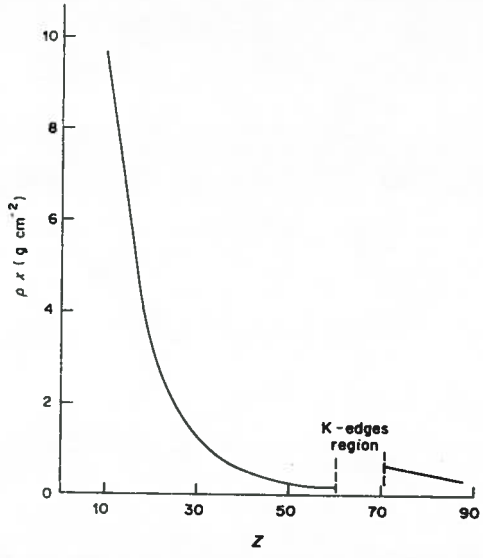

Fig. 5. Sample thickness critical values ρx vs the atomic number Z (see text).

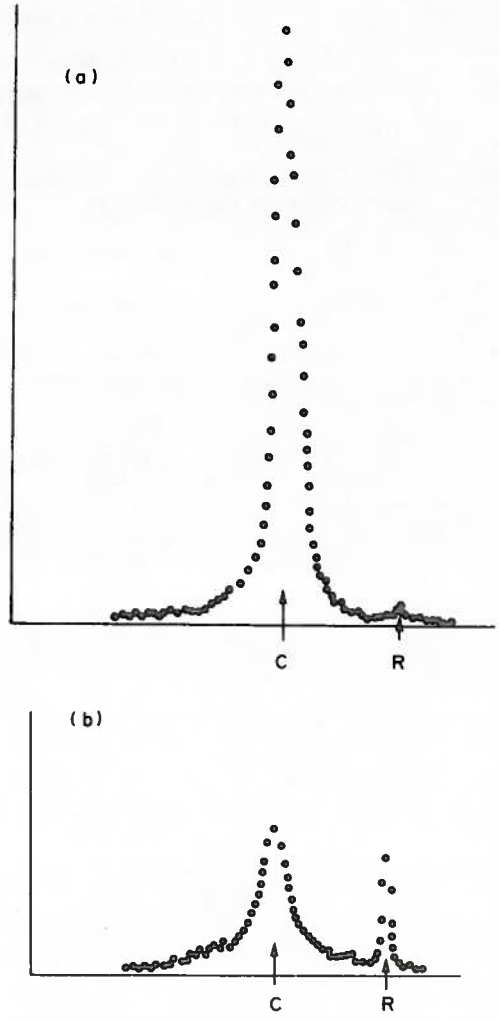

Fig. 6. Compton, C, and Rayleigh, R, peaks in the cases of low and medium Z materials: curve (a) graphite, curve (b) zinc.

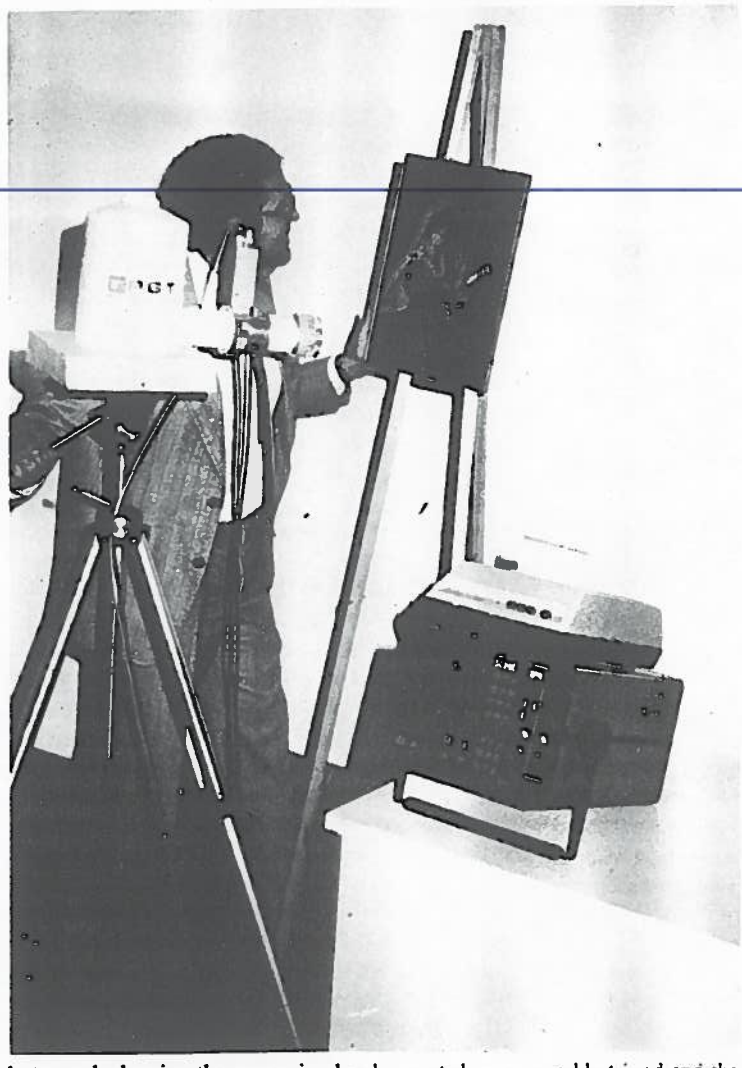

Fig. 1. A photograph showing the measuring head mounted on a movable tripod and the Scout MCA.

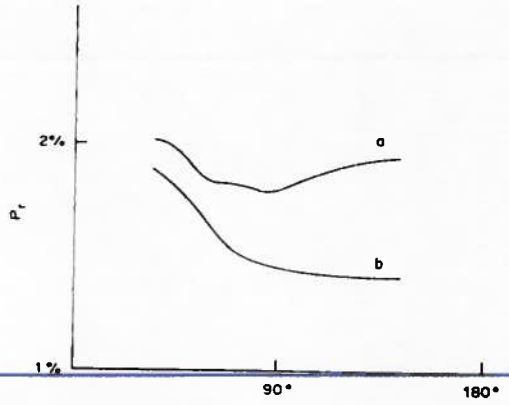

Fig. 2. The resolving power, P_r, vs the scattering angle ϑ for $29 \leqslant Z \leqslant 82$ curve (a) and for $6 \leqslant Z \leqslant 20$ curve (b). P_r is calculated at a constant Rayleigh count rate.

The choice of E_0 has been made according to the following requirements:

(i) low photoelectric cross-section for low-Z elements ($Z \leqslant 15$);

(ii) high photoelectric cross-section for medium and high-Z elements in order to attain a convenient XRF sensitivity;

(iii) a non-negligible sample excitation volume when highly absorbing materials are involved.

An energy such as that of the ^{241}Am γ-line at 59.5 keV turns out to fulfil the above-mentioned conditions. For instance the photoelectric-to-total cross-section ratio increases rapidly with Z, i.e. from 0.06 at $Z = 6$ to 0.43 at $Z = 15$. ^{241}Am sealed source can therefore be recommended for use in a multipurpose RCT–XRF spectrometer.

Generally speaking, a NDT device designed to inspect samples of any size, shape and geometry operates in the backscattering mode. The same holds for RCT with a diminution in the Rayleigh peak count rate and with the advantage of a complete energy separation of the two scattered components.

In order to evaluate quantitatively the RCT response function, we have plotted the resolving power* $P_r(w_i)$ vs ϑ at constant Rayleigh peak count rate as depicted in Fig. 2 where two different Z regions are considered. One sees that P_r does not get worse with increasing ϑ in the higher-Z region and is slightly better in the lower-Z region. We conclude that, provided satisfactory counting statistics are assured, backscattering geometry is preferred. In our multipurpose XRF–RCT spectrometer the measuring head, designed according to a 135° scattering angle, is therefore characterized by a very compact geometry. As stated above, longer measuring times are requested in order to compensate the lower elastically scattered γ-ray counting rates at large scattering angles. A 300–500 s counting time is in general sufficient to assure good statistics using two collimated 45 mCi ^{241}Am sources.

The measuring-head defines a volume in the analyzed sample according to the geometry depicted in Fig. 3. This volume can be defined as the intersection space of the cones related to the sources and counter collimators. The γ-ray sources surrounding the counter are arranged in such a way that the involved source-sample-counter distances are drastically minimized to the advantage of the count rate.

Experimental Results

In Fig. 4 the calculated R/C values[8] vs Z are reported for $E_0 = 59.5$ keV and $\vartheta = 135°$.

Almost two different regions can be considered. The low-Z region, characterized by a very high slope. is proportional to Z^4. The medium-high-Z region is characterized by a lower slope and is proportional to Z^2.

Different approximations must be applied according to whether the sample can be considered thin or thick.[2] In fact the sample thickness may introduce corrective factors due to self-absorption. In our working conditions the correction is negligible for $Z \leqslant 10$ as shown in Fig. 4, while for higher Z the correction due to "thick" samples is not negligible and increases with Z according to a rate approximately constant with respect to the "thin" sample curve. Further, in Fig. 4 some experimental R/C values dealing with pure elements are represented showing a very good agreement with the calculated curve behaviour.

It is important to note that the sample thickness explored with the RCT decreases dramatically as the

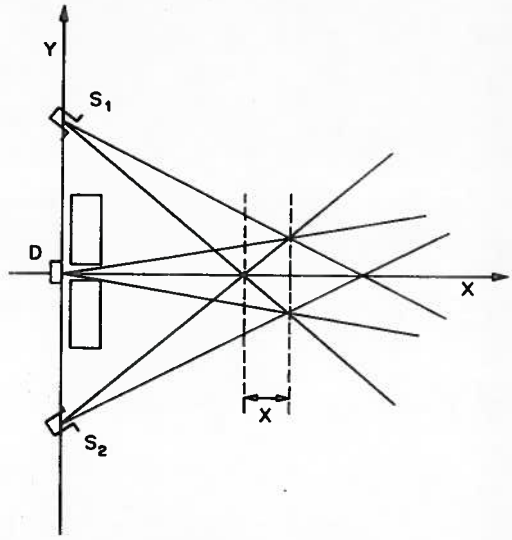

Fig. 3. Schematic representation of the measuring-head geometry. The analyzed volume is defined according to the apertures of collimators and depends on the sample mass absorption coefficient. S_1, S_2 sources, D detector.

* The relative resolving power $P_r(w_i)$ is given by[7]

$$P_r(w_i) = b\sqrt{2}\,\sigma_d\,[\partial d/\partial w_i]^{-1}$$

where $d = R/C$, σ_d is the statistical error over R/C and w_i is the weight fraction of the i-th element of a compound.

Int. J. Appl. Radiat. Isot. Vol. 35, No. 6, pp. 481–488, 1984
Printed in Great Britain.

0020-708X/84 $3.00 + 0.00

A Multipurpose Energy Dispersive x-Ray Spectrometer for Low, Medium and High-Z Materials Analysis*

GIOVANNI E. GIGANTE[1] and SEBASTIANO SCIUTI[2]

[1]Department of Biomedical Sciences, University of L'Aquila, Italy and [2]Department of Energetica, University of Rome "La Sapienza", Italy

(*Received* 1 *August* 1983)

An improved analytical technique simultaneously using the information from x-ray fluorescence and from the ratio Rayleigh/Compton (R/C) of elastic and inelastic scattered radiations is described.

The analyses are performed in a 135° scattering geometry by using two 45 mCi ^{241}Am point sources, a Ge–HP x-ray detector and a 2000 channel pulse height analyser.

The 135° scattering angle and the 59.5 keV ^{241}Am γ sources represent a convenient choice for a multipurpose spectrometer able to analyse very low-Z materials through the R/C ratio, and medium and/or high-Z materials through a XRF–R/C combination. The R/C ratio is able to give rapid synthetic information on the sample composition as shown in several examples concerning low-Z chemical compounds or mixtures and medium or high Z alloys. The spectrometer described and conceived for fast first-approach analyses is characterized by a 1% sensitivity in a measuring time of some 100 s.

As is well known energy dispersive x-ray fluorescence (XRF) technique is widely employed in many different fields in non-destructive elemental analyses.[1–3]

This technique is characterized by good analytical sensitivity and accuracy except when self-absorption is not negligible or when the analyses deal with matrices of unknown composition.

Fortunately, as will be pointed out, the scattering components in a XRF spectrum induced by a monochromatic γ-ray source of appropriate energy can overcome the above mentioned limitations.

In fact in the last decade energy resolution and detection efficiency improvements of x-ray solid state detectors has made possible the analysis of soft and hard x-rays. The scattered fractions of x-ray spectra excited by a monochromatic low-energy γ-ray source can be resolved and consequently an *ad hoc* designed spectrometer with energies above the fluorescence radiation energies shows elastic and inelastic scattered photons.

As shown by many authors[4–6] the most useful parameter related to these scattering processes turns out to be the ratio between the Rayleigh, or elastic, and the Compton, or non-elastic, peak areas R/C. Consequently an analytical technique referred to herewith as RCT (Rayleigh/Compton Technique) can be introduced.

RCT is characterized by quite a small dependence upon geometric factors and sample density. Further, RCT turns out to be a very useful tool complementary to XRF analyses. Therefore the most complete analytical assembly must be conceived as a XRF–RCT spectrometer. Such a spectrometer can be successfully employed in field measurements.

In this work optimization criteria in the design and construction of a measuring-head (source-detector assembly) for a multipurpose portable XRF–RCT spectrometer are described. The spectrometer has been assembled with the aim of carrying out analyses of materials in the fields of engineering, archaeometry and medicine.

Several experimental results are discussed in order to demonstrate the RCT performances

Instrumentation

The spectrometer is composed by currently used and reliable electronic devices and detectors, i.e. a Laben 2048 multichannel analyser, "Scout" and a Princeton Gamma Tech hyperpure planar Ge x-ray detector (FWHM 273 eV at 6.4 keV; 10 mm thickness) housed in a 2-L dewar ($\sim$ 10 h of autonomy) as shown in Fig. 1.

As stated above we have devoted our efforts to the design of the measuring-head, in order to optimize the spectrometer excitation and response functions. To this end we have critically examined the physical, instrumental and geometrical parameters such as the excitation γ-ray energy E_0 and the scattering angle ϑ.

*This research was supported in part by Consiglio Nazionale delle Ricerche (CNR) under Contract No. 82.00948.11.